Evanescent Wave-Based Particle Tracking Technique for Velocity Distribution in Extended Nanochannel

Y. Kazoe*, K. Iseki, K. Mawatari and T. Kitamori

*The University of Tokyo, Tokyo, JAPAN, kazoe@icl.t.u-tokyo.ac.jp

ABSTRACT

Understanding fluid flows in extended nanospace (10-1000 nm) is a fundamental issue to develop novel nanofluidic systems. The present study measured pressure driven flows in a 400 nm fused silica nanochannel by 100-300 kPa. A nanoscale particle tracking method using 64 nm fluorescent nanoparticle and the evanescent wave with total internal reflection of laser beam was developed to obtain the flow profile. The particle position in the nanochannel was determined from the fluorescent intensity, which is proportional to the evanescent wave intensity decaying exponentially from the wall. In order to reduce an error by the Brownian diffusion of tracer nanoparticles, the time resolution of the particle tracking was reduced to 260 μs. Flow velocity in the nanochannel, which is much smaller than the optical diffraction limit, was successfully obtained. This study provides basic knowledge of fluid and mass transport in nanospace.

Keywords: nanochannel, evanesent wave, nanoparticle, fluid flow, velocimetry

1 INTRODUCTION

Micro chemical system is a rapidly expanding engineering field and now focusing on nanofluidics. For the space of 1-10 nm, the dominant interactions between surface and molecules due to large surface-to-volume ratio affect liquid structure, and yield unique properties such as higher viscosity and higher conductivity compared to the bulk [1, 2]. Recently, these liquid properties also have been reported for 10-1000 nm space, i.e., extended nanospace [3, 4]. NMR studies revealed higher proton mobility and proposed a model of proton transfer phase where water molecules are loosely coupled near the surface of 50 nm [5]. In addition to these properties, unique ion transport phenomena are also generated by dominant electrostatic force caused by the electric double layer of 1-100 nm [6-8]. Therefore this space has potential of novel devices for energy production, chemical synthesis and biochemical analysis using these specific properties.

However, fluid dynamics in the nanoscale, which is a fundamental component for development of the devices, has not been revealed. Previous work investigated nanochannel flows using streaming potential [9, 10], current monitoring [11], molecular tagging technique and numerical simulation [12], but it has been difficult to directly measure the flow structure and material transport.

One potential approach is to use evanescent wave-based optical measurement technique which can overcome the Abbe's diffraction limit. Nano particle tracking velocimetry (nPTV) using fluorescent tracer particles and the evanescent wave has been developed to investigate near-wall flows and particle behavior in microchannels [13-15]. Most recently, the technique was developed to obtain the near-wall flow profile, particle distribution and diffusion coefficients [16-18]. Since the evanescent wave has an exponential decay as function of the distance from the surface with the order of 100 nm, the position of the tracer particles could be determined from the fluorescent intensity. However, the size of tracer particles is of order of 100 nm and it is difficult to be applied to 100 nm order nanochannels.

The present study therefore measured pressure driven flows by 100-300 kPa in a fused-silica nanochannel of 410 nm depth, 50 μm width and 400 μm length. The method was developed for measurements of nanochannel flows by using 10 nm order nanoparticles. In case of using the tracer nanoparticles, previous studies have reported that asymmetric Brownian diffusion by an additional hydrodynamic drag due to the wall induces bias errors [19, 20]. Especially in the nanochannels, the effect of the Brownian diffusion may be more significant, since the diffusion displacement is comparable to the channel size. Hence the time resolution of particle tracking was decreased to order of 100 μs, in order to suppress the diffusion to the size comparable to the nanoparticles. The velocity profile in the nanochannel was successfully obtained.

2 EXPERIMENTAL SECTION

2.1 Materials and Chemicals

$Na_2B_4O_7$ 1 mM (pH = 9.0) was prepared as working fluid. Carboxylate-modified fluorescent polystyrene particles of a 64 ± 7 nm diameter, which was evaluated by dynamic light scattering technique, were used as the tracer and seeded into sample solutions with a volume fraction of 0.0002%. The zeta potentials of nanoparticles ζ_p was evaluated to be using a Zetasizer (Malven Instuments).

2.2 Fabrication of Nanochannel

The fabrication of microchip containing nanochannels has been described previously [21]. The nanochannels were

fabricated on a fused-silica plate by electron beam lithography and plasma etching. The width and depth of the nanochannels were measured by scanning electron microscopy and atomic force microscopy, respectively. After fabricating the nanochannels, microchannels for the sample injection were fabricated on a same glass plate. Then holes for inlets and outlets were made, and the channels were sealed with another fused silica plate of a 0.17 mm thickness by thermal fusion bonding. Prior to the experiments, the channel was cleaned by flashing acetone, ethanol, deionized water, 10^{-1} mol/L potassium hydroxide (KOH), and then rinsed by deionized water. The sample solution was driven by an air pressure control system and injected into a microchannel of 500 μm width and 5 μm depth for sample injection, and then into the nanochannel, as illustrated in Figure 1. The zeta-potential of fused silica wall ζ_w were also evaluated to be using SiO_2 particles of a 500 nm diameter.

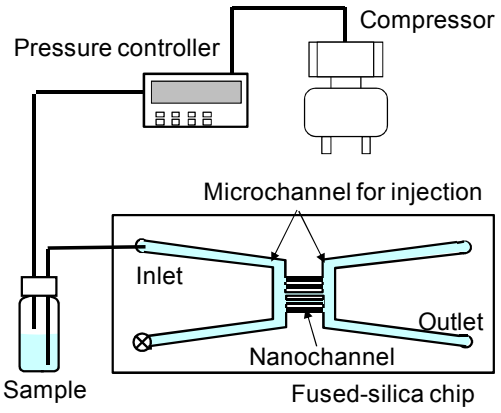

Figure 1: Schematic of pressure control system.

2.3 Measurement System

The nanoparticles flowing through the nanochannel were imaged by an evanescent wave illumination system with total internal reflection of a 532 nm laser beam as illustrated in Figure 2. The laser beam was converted to two laser pulses, each 190 μs width and separated by 70 μs, using an acoustic optic modulator, and introduced into the microchip through a prism. Then fluorescence excited by the evanescent wave was corrected through an objective lens (60×, NA = 1.42) and an emission filter passing wavelengths over 570 nm, and 1500 image pairs of 136 μm × 27 μm (512 pixel × 100 pixel) at Δt = 260 μs were captured by an EMCCD camera, which was synchronized with the laser pulses. Hence the Brownian displacement of nanoparticles given by $(2D_\infty \Delta t)^{1/2}$ was decreased to 60 nm smaller than the particle size considering the hinderance by the wall, where D_∞ is a diffusion coefficient described by the Stokes-Einstein relation.

After correcting a camera nonlinearity, location of particles in the nanochannel was determined using the images (Figure 2(c)). After removing image noise by a Gaussian filter, the location of the particle centers was determined by the cross-correlation of the particle images with a 2D Gaussian function. Then the particle edge-wall distance h was estimated based on an assumption that the particle image intensity I_p is proportional to an exponential decay of the evanescent wave, $I_p \propto \exp(-h/z_p)$ where z_p is the penetration depth of the evanescent wave. Using two particle image intensities stuck on the two walls as references, the particle edge-wall distance is given by

$$h = (H - 2a)\frac{\ln I_p - \ln I_1}{\ln I_2 - \ln I_1} \qquad (1)$$

where I_1 and I_2 are partice image intensities stuck on the wall at $h = 0$ and $h = H - 2a$, respectively (H is the channel

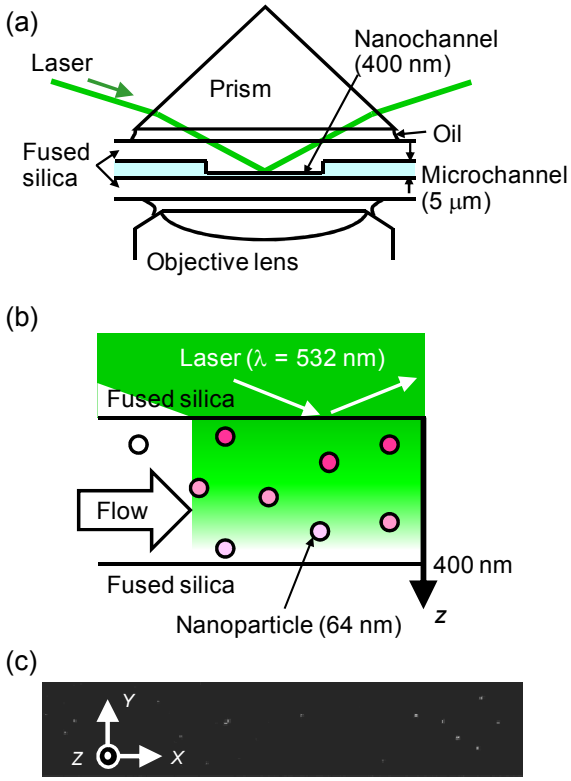

Figure 2: Schematics of (a) prism-based optical system and (b) evanescent wave illumination in nanochannel. (c) Fluorescence image of nanoparticles.

depth and a is the particle radius). Then the position of the particle center was determined as $z = h + a$. The penetration depth of the evanescent wave was evaluated to be z_p = 141 ± 8 nm. The uncertainty of the particle position was 33 nm by errors by the noise in the fluorescence detection of 23 nm, the penetration depth of 0-7 nm and particle diameter of 3.5 nm.

3 RESULTS AND DISCUSSION

Figure 3 shows profiles of the particle number density as fuction of the wall normal position z. The partilce number densities have symmetric profiles but some particles are detected inside the wall owing to an error of the normal position z. The particles in the nanochannel have nonuniform distribution and are concentrated in the center of the nanochannel around z = 200 nm, because of the dominant electrostatic repulsion between negatively charged walls and particles. The region of particle depletion is much broader than the Debye shelding length of 6.8 nm. This suggests that the electrical polarization in nanospace is more significant than microspace due to breaking electroneutrality by dominant surface effects. In addition, the profiles of particle number density are almost independent of the applied pressure into the nanochannel. This indicates that the lift force on the nanoparticle by the shear stress in pressure driven flow is negligeble in the particle behavior.

Based on the particle behavior, region of the velocity measurement by the tracer displacement was discussed. The data can not be obtained for z < 32 nm because the particle center can not go to the wall owing to its size. Also, the number of the particle in the vicinity of the wall is not sufficient owing to the depletion by the electrostatic repulsion. Therefore, measurement region of the velocity profile was estimated to be 64 nm < z < 346 nm.

Figure 4 shows the velocity profiles of pressure driven flow in the nanochannel. The velocity profile in the nanochannel was successfully obtained. The velocities increase with increasing the applied pressure and become maximum around the center of the nanochannel at z = 200 nm in approximately agreement with the Hagen-Poiseulle flows. From the fitting curve to the velocity profiles, the results suggest that slip velocities appear in the nanochannel, even for the hydrophilic fused silica surface. However, owing to the Brownian velocity, the measured velocities have fluctuation of around 0.5 mm/s. This will significantly can affect the accuracy of the measurement for estimation of the near-wall profiles. Future work investigates the effect of the Brownian diffusion more precisely, by changing particle size and time resolution.

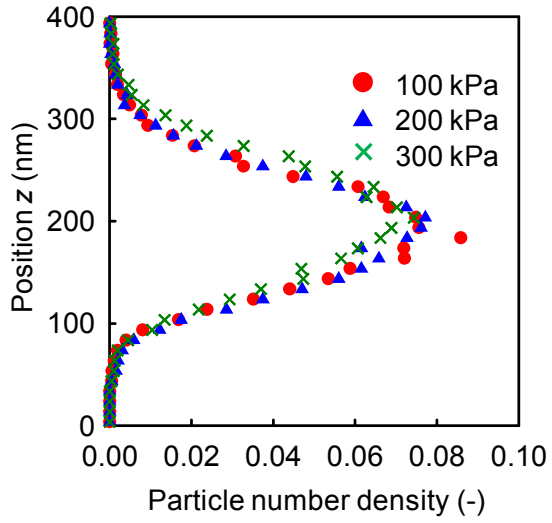

Figure 3: The particle number density as function ot the position z.

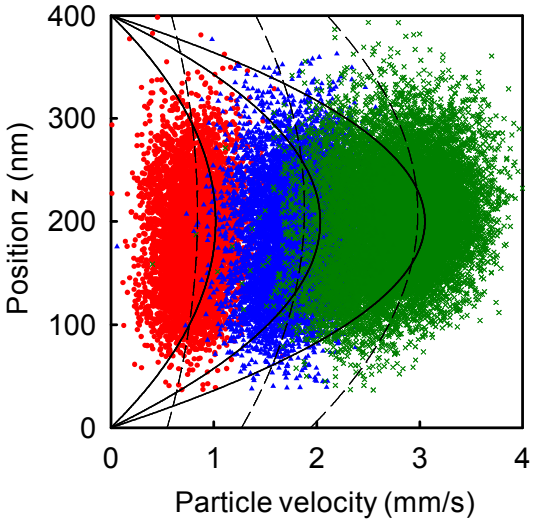

Figure 4: The particle velocities of pressure driven flow as function ot the position z. Solid lines show theoretical values of the Hagen-Poiseulle flow. Dashed lines show fitting curves to the experimental results.

4 CONCLUSION

We reported measurement of pressure driven flows in a 400 nm extended nanochannel using evanescent wave-based particle tracking velocimetry. The method was developed for the nanochannel flows by using 64 nm nanoparticles and decreasing the time resolution to suppress the Brownian diffusion. The Brownian diffusion of nanoparticles was supressed to 60 nm comparable to the particle size. Measurement with the uncertainty of the particle position of 33 nm, which is smaller than the particle diameter, was achieved by the fluorescence detection system. This study provides fundamental knowledge of fluid and mass transport in the nanochannel and will contribute to development of nanofluidic systems for single molecule analysis, chemical synthesis and energy harvesting.

5 ACKNOWLEDGEMENT

This work was supported by a Grant-in-Aid for Specially Promoted Research from the Japan Society for the Promotion of Science (JSPS). We thank Dr. K. Miyata in

Graduate School of Medicine at the University of Tokyo for the Zetasizer measurements.

REFERENCES

[1] J. Haneveld, N. R. Tas, N. Brunets, H. V. Jansen andM. Elwenspoek, J. Appl. Phys., 104, 014309, 2008.
[2] C. Duan and A. Majumdar, Nature Nanotech., 5, 2010.
[3] K. Mawatari, T. Tsukahara, Y. Sugii and T. Kitamori, Nanoscale, 2, 1588, 2010.
[4] A. Hibara, T. Saito, H.-B. Kim, M. Tokeshi, T. Ooi, M. Nakao and T. Kitamori, Anal. Chem., 74, 6170, 2002.
[5] T. Tsukara, A. Hibara, Y. Ikeda and T. Kitamori, Angew. Chem. Int. Ed., 46, 1180, 2007.
[6] D. Stein, M. Kruithof and C. Dekker, Phys. Rev. Lett., 93, 035901, 2004.
[7] Y. Kazoe, K. Mawatari, Y. Sugii and T. Kitamori, Anal. Chem., 83, 8152, 2011.
[8] Q. Pu, J.Yum, H. Temkin and S. Liu, Nano Lett., 1099, 2004.
[9] F. H. J. van der Heyden, D. Stein and C. Dekker, Phys. Rev. Lett., 95, 116104, 2005.
[10] Y. Xie, X. Wang, J. Xue, K. Jin, L. Chen and Y. Wang, Appl. Phys. Lett., 93, 163116, 2008.
[11] P. Mela, N. R. Tas, E. J. B. Berenschol, J. van Nieuwkasteele and A. van der Berg, Electrophoresis, 25, 3687, 2004.
[12] S. Pennathur and J. G. Santiago, Anal. Chem., 77, 6782, 2005.
[13] C. M. Zettner and M. Yoda, Exp. Fluids, 34, 115, 2003.
[14] J. S. Guasto, P. Huang and K. S. Breuer, Exp. Fluids, 41, 869, 2006.
[15] S. Pouya, M. Koochesfahani, P. Snee, M. Bawendi and D. Nocera, Exp. Fluids, 39, 784, 2005.
[16] H. F. Li and M. Yoda, J. Fluid Mech., 662, 269, 2010.
[17] Y. Kazoe and M. Yoda, Langmuir, 27, 11481, 2011.
[18] Y. Kazoe and M. Yoda, Appl. Phys. Lett., 99, 124104, 2011.
[19] P. Huang, J. S. Suasto and K. S. Breuer, J. Fluid Mech., 637, 241, 2009.
[20] R. J. Hunter, “Zeta Potential in Colloid Science”, Academic Press, London, 1981.
[21] T. Tsukahara, K. Mawatari, A. Hibara and T. Kitamori, Anal. Bioanal. Chem., 391, 2745, 2008.